Strain-compensation in closely-stacked quantum dot active regions grown by metal organic chemical vapor deposition

N. Nuntawong, J. Tatebayashi, P. S. Wong, Y. C. Xin, C. P. Hains, S. Huang,
L. F. Lester and D. L. Huffaker[*]
Center for High Technology Materials, University of New Mexico,
1313 Goddard SE, Albuquerque, NM, USA 87106

ABSTRACT

In this paper, we describe the results of using strain-compensation (SC) for closely-stacked InAs/GaAs quantum dot (QD) structures. The effects of the (In)GaP SC layers has been investigated using several methods. High-resolution x-ray diffractometry (XRD) quantifies the values of experimental strain reduction compared to calculations. Atomic force microscopy (AFM) indicates that the SC layer improves both QD uniformity and reduces defect density. Furthermore, increase in photoluminescence (PL) intensity has been observed from compensated structure. The use of Indium-flushing to dissolve large defect islands prevent further defect propagation in stacked QD active region. Room-temperature ground-state lasing at emission wavelengths of 1227-1249 nm have been realized with threshold current densities of 208-550 A/cm^2 for 15-20 nm spacing structures.

Keywords: quantum dot, strain compensation, InAs, GaAs, InGaP, MOCVD, MOVPE

1. INTRODUCTION

Quantum dot (QD) material systems have drawn considerable interest due to the optoelectronic advantages that zero-dimensional systems offer. Using molecular beam epitaxy (MBE), impressive properties such as low threshold current,[1] low threshold current density,[2] and high characteristic temperature[3] of room-temperature (RT) continuous-wave lasers at 1.3 μm have been demonstrated. In comparison, there have been relatively few reports of 1.3-1.5 μm emission from QDs grown by metalorganic chemical vapor deposition (MOCVD). While shorter wavelength (1.1-1.3 μm) MOCVD-grown lasers have been demonstrated,[4-5] extending the wavelength for MOCVD-grown QDs is challenged by increased compressive strain due to higher Indium composition coupled with shortened surface adatom migration lengths in MOCVD growth.[6-7] Another difficulty of the 1.3 μm QD structure is the small gain in the ground state of an active region. The gain can be increased by stacking InAs/GaAs QD layers, however, accumulated overall strain in the epitaxial material can degrade PL efficiency and produce non-radiative recombination center due to dislocation. Several groups have reported stacking the QD layers to increase modal gain near 1.3 μm[8-10] resulting in ground-state lasing and larger T_o. However, accumulated overall strain in the epitaxial material can cause defects and non-radiative recombination centers that increase the threshold current density and cause device failure. A thick spacer (300 Å to 500 Å) between the QD layers is often used to reduce strain accumulation and defects. However, the extended active region reduces the optical overlap and is not attractive for microcavity lasers such as vertical-cavity surface-emitting lasers (VCSEL) where spacing thickness between active regions should be minimized. The accumulated strain in closely stacked structure can be relieved by using SC technique. Use of strain-compensation (SC) layers has been successful in stacking multiple strained quantum wells (QWs) in heterostructure laser.[11-13] The use of SC layers to reduce strain in stacked QD active regions may be a powerful parameter in designing QD laser structures. The compensation of compressive strain by inserting tensile layers has been successfully demonstrated using InGaP and InGaAsP in multiple QWs lasers. Although accumulated strain is a severe limitation in stacked QD actives, there has been surprisingly few report of SC in QD structures. This is likely due to the inconvenience of a pyrophoric phosphide source in QD-growing MBE systems. In this article, we will discuss the results of using thin tensile InGaP layers embedded in GaAs barrier layers and demonstrate the reduction of accumulated strain, as well as improvement of dots uniformity that affect the optical properties of laser devices.
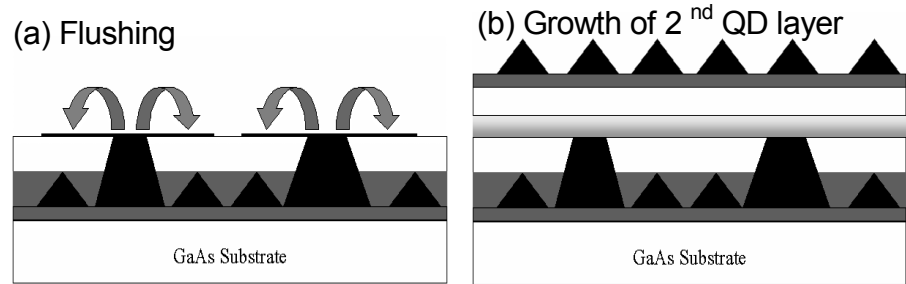
---

[*] huffaker@chtm.unm.edu; Phone 1 505 272-7845; Fax 1 505 272-7801

2. GROWTH OF STRAIN-COMPENSATED STACKED SAQD BY MOCVD

Our samples are grown by MOCVD at 60 Torr using trimethylgallium, trimethylindium, trimethylaluminum, tertiarybutylphoshine and arsine (AsH_3). Growth is initiated on a GaAs (001) substrate with a 3000 Å GaAs layer at 680 °C, then the temperature is reduced and stabilized for active region growth within the range of 450-520 °C. All active regions consist of a 5 ML $In_{0.15}Ga_{0.85}As$ buffer layer, a 3 ML InAs QD coverage, and a 25 ML $In_{0.15}Ga_{0.85}As$ cap. A post nucleation AsH_3 pause[14] is used after the growth of each QD layer to reduce the defect density. The stacked QD layers are separated by a 15~20 nm GaAs barrier sandwiching the 4~8 MLs $In_xGa_{(1-x)}P$ SC layer. The thicknesses of SC layers are measured from high-resolution transmission electron microscopy (TEM) images. The interface regions, GaAs/(In)GaP and (In)GaP/GaAs, are optimized through the switching of gas flows to minimize Indium segregation and As-P interchange.

To used the effect of further defect reduction in SC structures, additional Indium-flushing step (AsH_3 pause) is initiated in another set of sample, in Fig. 1(a), at the same growth temperature. During this step, all sources are switched off, including AsH_3, allowing the Indium atoms from large uncapped defect cluster to diffuse along the GaAs surface and evaporate from the structure. The optimized pause time for

Figure 1. Schematic illustrations of the growth step of the active region by using defect dissolution technique to reduce defect formation.

this step is 90 s. Growth is resumed with a 4 ML GaP SC layer and another GaAs barrier followed by the next InAs QD layer shown in Fig. 1(b). The remaining Indium atoms on GaAs surface are trapped in GaP SC layer. For this study, a total of five QD stacks are grown in this manner and finally capped with 80 nm of GaAs. The details of optimizing this defect reduction method have been described in our previous work. [15]

Finally, laser structures are grown on n-type substrates followed by a 300 nm GaAs n^+ doped buffer, a 0.8 μm n-$Al_{0.7}GaAs$ (n ~1 × 10^{17} cm^{-3}) lower clad, a 110 nm GaAs waveguide embedding the active region, and a 0.8 μm p-$Al_{0.7}GaAs$ (p ~1 × 10^{17} cm^{-3}) upper clad. The structures are terminated with a 50 nm GaAs p^+ layer.

3. RESULTS AND DISCUSSIONS

3.1 Strain reduction in stacked structures

A series of 5-stacks samples with varied Indium content in $In_xGa_{1-x}P$ SC layers ranged from x=0 to x=0.36 have been grown for HRXRD and RTPL characterization. By varying SC thickness from 2 ML to 8 ML, the optimized thickness which gives maximum RTPL intensities of each SC composition has been obtained. Experimental symmetric scans around (004) reflection in $\omega/2\theta$ geometry are used to measure the effect of SC layers on the strain accumulation and lattice distortion in tested structures. Resulting data of samples embedded with optimized SC thickness is summarized in Table I for four samples that have 5-stack actives with spacing thickness of 15 nm. Examples of x-ray diffractometry (XRD) spectra from 5-stack with (a) no SC, (b) 8 ML $In_{0.36}GaP$, (c) 8 ML $In_{0.36}GaP$ and (d) 4ML GaP structures are shown in Fig. 2. The three spectra are characterized by zero-order peaks located at (a) $\Delta\theta = -1962$ arcseconds (b) $\Delta\theta = -1476$ arcseconds (c) $\Delta\theta = -1283$ arcseconds and (d) $\Delta\theta = -1264$ arcseconds. The zero-order peaks in Fig. 2 (b) , (c) and (d), shift closer to the GaAs substrate peak and indicate reduced compressive strain with decreasing In content in the SC layers. The average perpendicular strain, $<\varepsilon_\perp>$ can be determined by [16]
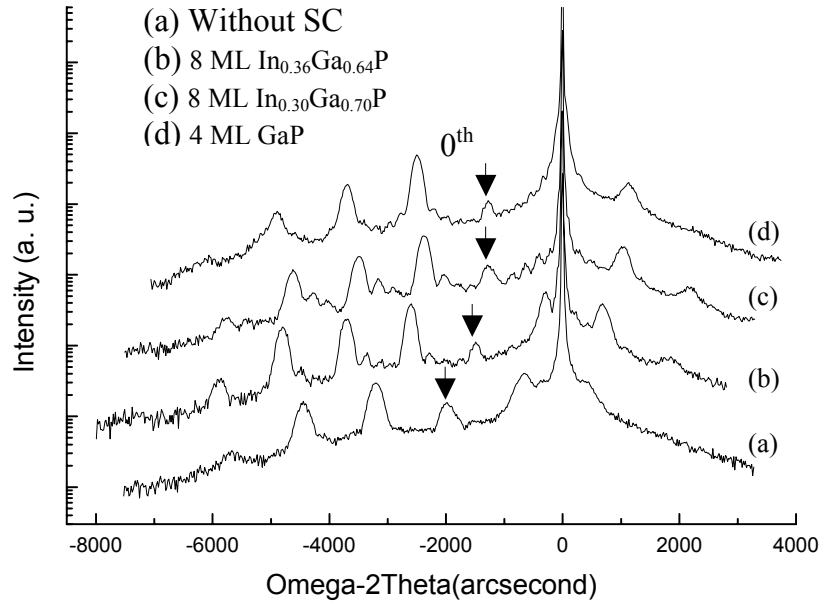
Figure 2. Symmetric 004 x-ray diffraction patterns for a 5-stack QD structure with (a) no SC layer, (b) 8 ML In$_{0.36}$GaP, (c) 8 ML In$_{0.36}$GaP and (d) 4 ML GaP.

$$\langle \varepsilon_\perp \rangle = \frac{\sin \theta_B}{\sin(\theta_B + \Delta\theta)} - 1 \tag{1}$$

where θ_B is the Bragg angle of the GaAs substrate. From equation (1) and experimental values for $\Delta\theta$, we calculate the total strain in each sample and list them in Table I. For the 5-stack, the total strain, $\langle\varepsilon_\perp\rangle$, varies from 0.014897 (no SC) to 0.00968 (4 ML GaP). These strain values indicate a 25% to 36% reduction in compressive strain due to SC layers compared to the sample without SC layers. The total average strain values for each sample were obtained from XRD spectra quantifies total average strain reduction by a factor of 36% with 4 MLs GaP compared with a structure without SC layer. The result is consistent with the calculated average perpendicular strain from [17]

$$\langle \varepsilon_\perp \rangle = \frac{\varepsilon_{active} t_{active} + \varepsilon_{SC} t_{SC}}{t_{active} + t_{SC}} \tag{2}$$

where $\varepsilon_{active,SC}$ and $t_{active,SC}$ are strain and thickness of QD active and SC layers, respectively.

In order to avoid fully relaxation, the total elastic energy, E_{total}, of the structure must be less than the critical elastic energy, E_c. The relation between total elastic density as function of stacking number, N_{stacks}, and average strain can be written as [18]

$$E_{total} \propto N_{stacks} < \varepsilon_\perp >^2 t_{spacing} \tag{3}$$

Based on amount of strain reduction, the total elastic energy can be reduced up to 60%. In other word, critical thickness of full structure can be extended by approximately factor of 2.

Data	No SC	In$_{0.36}$GaP (8 ML)	In$_{0.30}$GaP (8 ML)	GaP (4 ML)
$\Delta\theta$ (arcs)	-1962	-1476	-1283	-1264
$<\varepsilon_t>$	0.014897	0.01116	0.00968	0.00952
strain reduction(%) (Experiment)	---	25	35	36
strain reduction(%) (Calculated)	---	33	39	35

Table 1. Tabulated XRD data including zero-order peak, total strain, % strain reduction for 5-stack with spacer thickness of 15 nm.

3.2 PL properties
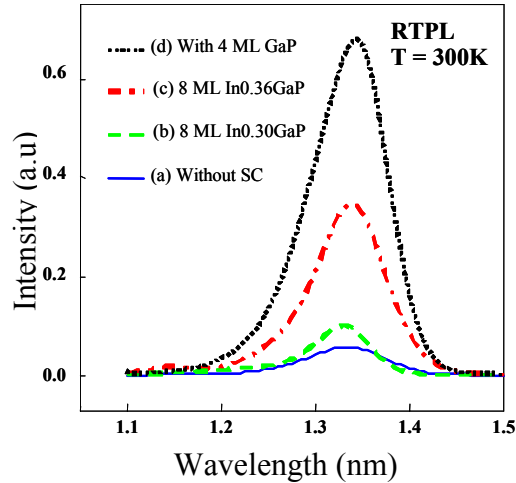
Figure 3. RT PL spectra comparing QD active regions with and without SC layers in 5-stack sample.

Figure 3 shows RTPL spectra of structures embedded with optimized SC layers thickness for each Indium content sample. The emission wavelengths at RT are observed between λ= 1340 nm and λ= 1325 nm. A comparison of the 5-stack PL spectra in this figure shows the PL intensity with SC is increased by factor of 1.8 (8 ML In$_{0.36}$GaP), 6.2 (8 ML In$_{0.30}$GaP) and 12.5 (4 ML GaP) compared to the uncompensated sample as a result of fewer non-radiative recombination centers. The FWHM varies slightly from sample to sample within a range of 58 to 70 meV. One of the interesting point in PL spectra is comparison between PL intensities of sample (c) and (d). Although these two sample have a similar amount of strain reduction, PL intensity of sample (d) is brighter than sample (c) by about factor of 2. This is most likely due to the difference in material uniformity of SC layers between InGaP and GaP due to indium segregation issue, which will be discussed in following section.

3.3 Spatial phase formation

Figure 4 (a) shows a high-resolution cross-sectional TEM image of the surface QD and its nearby In$_{0.36}$Ga$_{0.64}$P SC layer and GaAs spacer layer in sample A where the hexagonal phase has nucleated on the SC layer / GaAs interface.
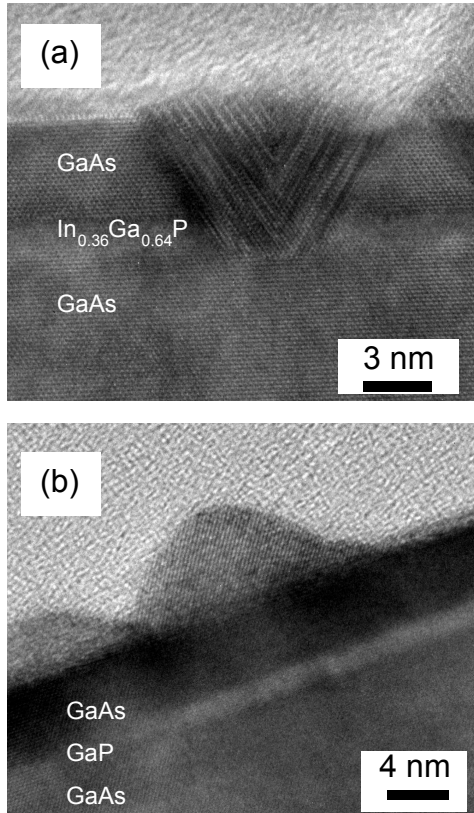
Figure 4. Cross-sectional TEM images of (a) hexagonal phase formation within structure with 8 ML $In_{0.36}Ga_{0.64}P$ SC layer, and (b) QD formation of structure with 4 ML GaP SC layer.

It is obvious that a dark contrast has been exhibited along the epitaxial layer after inserting the tensile $In_{0.36}Ga_{0.64}P$ layer.[19] The dark contrast in the InAs QDs is generally due to two aspects: i) the heavier element indium within QDs [20], and ii) strain contrast associated with lattice mismatch between QDs and spacer layer.[21] The major reason is due to chemical and structural driving forces. Firstly, from the point of chemical driving force, indium is comparatively rich in InAs QD layer than $In_{0.36}Ga_{0.64}P$ SC layer, which indium can diffuse from high concentration to low concentration. Secondly, from the point of structural driving forces, when GaAs grows on InAs, the lattice spacing of GaAs will enlarge due to its tensile effect compared to InAs, which open a channel for large Indium atom to diffuse into $In_{0.36}Ga_{0.64}P$/GaAs interface. It is the spacious $In_{0.36}Ga_{0.64}P$/GaAs interface that large Indium atom tends to stay once it diffuses in. Therefore, under the combined effect of chemical and structural forces, Indium atoms could diffuse and stay around GaAs/SC interface, where the InAs hexagonal phase nucleation starts. Since the cubic {111} facets have the same closed-packed properties as the hexagonal {0001} facets, continued growth of InAs on this structure begins selectively on the GaAs {111} facets and extends its hexagonal phase on {0001} facets. The hexagonal phase formation is absent for structure with 4 ML GaP SC layers as shown in Fig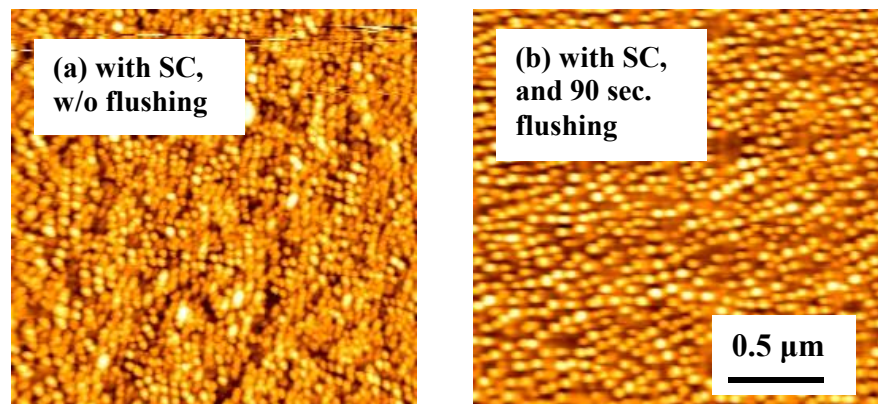ure 4 (b). This is most likely due to lower strain contrast within this structure compare to the structure with InGaP SC which known having Indium segregation issue.

The effect of hexagonal phase material present in active regions on optical characteristics is still unclear. In general, high dot uniformity with a low defect density is important factors for laser devices. The hexagonal phase material may act as non-radiative recombination center which is not preferable. From this reason, using GaP material for SC layers in active region is more suitable for stacked QD structure.

3.4 Defect dissolution

In the previously reported Indium-flushing method,[23] island dissolution is accomplished by increasing the wafer temperature by approximately 100 °C just after the InAs QDs are capped with a thin GaAs barrier. During this anneal, the capped InAs QDs are completely covered by the GaAs

Figure 5. AFM images (2 μm × 2 μm) of surface QDs (a) with 4 ML GaP SC layers without In-flush and (b) with SC layers and a 90 sec In-flush.

barrier and remain intact, while the large InAs defect clusters are exposed to the surface and will be partially evaporated. The disadvantage of this method is the In/Ga intermixing driven by the increased temperature that results in large blue shift and degraded emission efficiency.[24]

In this work, we characterize the formation of surface QDs grown atop a 15 nm spacing thick 5-stack active region with and without the Indium-flushing step. Figure 5 shows AFM images (2 μm × 2 μm) of surface QDs (a) with 4 ML GaP SC layers without Indium-flush and (b) with SC layers and a 90 s Indium-flush. The 5-stack sample (a) without Indium-flush has a high defect density of 5×10^8 /cm^2 regime which is comparable to single stack QD. The addition of Indium-flush along with SC layer, as in Fig. 5(b), results in significantly higher material quality and a QD ensemble free of coalesced islands. From comparing QD size in Fig. 5(a) and (b), we see that the average QD size is not strongly affected by the Indium-flushing step and remains stable in width (~ 35 nm) and height (~ 7.5 nm) with QD density ~ 5×10^{10} QDs/cm^2 for both structures. The average QD size increases by ~10% in width and ~35% in height compared to single QD layer.

Figure 6 shows 3-dimensional surface morphology of the three structures of the 5-stack QD structure with different flushing times obtained from (1 μm × 1 μm) AFM images, (a) without flushing (RMS roughness = 1.251 nm), (b) with 90 s flushing (RMS roughness = 0.626 nm), and (c) with 150 s flushing (RMS roughness = 0.114 nm). The flushing steps result in a significantly smoother surface as the crystalline defect density is reduced. The RMS roughness decreases linearly from 1.251 nm to 0.114 nm as the flush time is increased from 0 s to 150 s and corroborates a
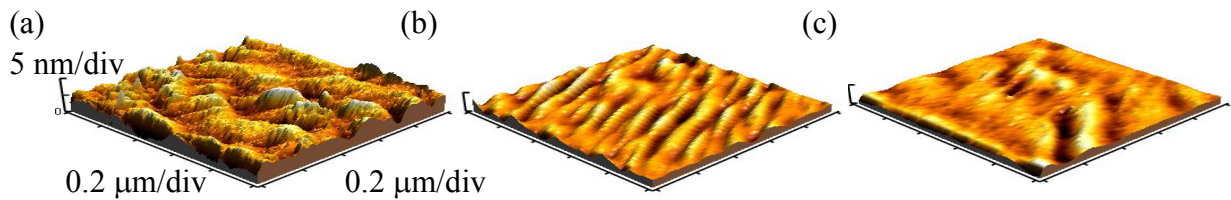
Figure 6. 3-dimensional surface morphology of the three structures of the 5-stack QD structure with different flushing times obtained from (1 μm × 1 μm) AFM images, with (a) without flushing (RMS roughness = 1.251 nm), (b) 90 sec flushing (RMS roughness =0.626 nm), and (c) 150 sec flushing (RMS roughness =0.114 nm).
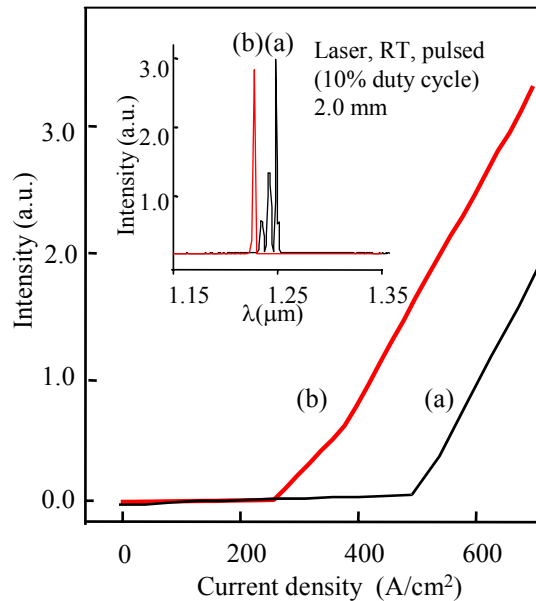
Figure 7. L-I characteristic and lasing spectra for (a) 3-stack QD lasers and (b) 6-stack QD lasers with 4 ML GaP SC layers.

reduced defect density in the structure. Without Indium-flushing, an undulating surface is visible and with Indium-flushing the surface is atomically smooth. The improved surface morphology is expected to significantly reduce optical internal loss in the laser structure.

3.5 Strain compensated laser devices

Finally, we demonstrate lasers that utilize a 3-stack and 6-stack InAs QD active with 4 ML GaP embedded in a GaAs matrix. Figure 7 shows the output power-current [L-I] characteristics and lasing spectra at RT under pulsed conditions (10% duty cycle) for (a) a 3-stack and (b) 6-stack InAs QD active. The light versus current curve indicates (a) J_{th}=550 A/cm^2 and (b) J_{th}=208 A/cm^2, the inset shows a multi-mode lasing spectrum centered at (a) λ=1.249 μm and (b) λ=1.227 μm. The broad area laser dimensions are 50 μm × 2 mm. High reflectivity coatings (3 pairs Si/Al$_2$O$_3$) are applied by a sputtering technique to both facets of the fabricated lasers. Ground-state lasing of the fabricated lasers with uncoated facets is not obtained due to insufficient gain. This allows us to place upper and lower boundaries on the 3-stack modal gain. We estimate 3-stack modal gain to be approximately 8 cm^{-1} and 10 cm^{-1} for 6-stack based on an internal loss of about 5 cm^{-1} for MOCVD grown QD laser.[25] We observe a 45~55 nm blue-shift of the lasing peak compared to the RTPL spectra (Fig. 3(a)) which indicates saturation of the larger QDs at high injection current such that lasing transitions originate from smaller QDs.[26]

4. CONCLUSIONS

In conclusion, we have characterized the effect of SC layers in closely stacked InAs QD structures grown by MOCVD. Our structures are comprised of thin (In)GaP SC layers in 15~20 nm spacing thickness SC in stack QD actives. From XRD characterization, the SC layers reduce the cumulative strain in a 5-stack by over 36%. The reduced overall strain leads to reduced non-radiative recombination centers and greatly improved PL properties in stack QD structure. The results suggest that using binary GaP for SC layer is more preferable than ternary InGaP compound due to lower strain contrast within the structure.

We also report a technique for defect reduction in closely stacked QD active regions by introducing an Indium-flushing step in combination with GaP SC layers. The GaP SC layers reduce residual strain propagation allowing a dense QD stack and the Indium-flush reduces the density and propagation of defective islands that are common in MOCVD growth. The Indium-flush described in this work effectively dissolves the defective islands via an AsH$_3$ pause rather than an anneal step that also shortens the emission wavelength. Both improved morphology and low defect structures suggest that this growth technique is suitable for long wavelength emission laser applications. Furthermore, the QD layer separation of only 15~20 nm will produce an attractive active region for VCSEL applications.

RT ground-state lasing at λ= 1.227-1.249 μm, J_{th} = 208-550 A/cm^2 have been demonstrated from strain compensated QD active regions. This data suggests that SC layers can be used to improve the performance of stacked QD actives in lasers by increasing modal gain and reducing internal loss.

5. ACKNOWLEDGEMENTS

REFERENCES

1. A. Stintz, G. T. Liu, L. H., L. F. Lester, and K. J. Malloy, IEEE Photonics Technol. Lett. **12,** 591 (2000).
2. G. Park, O. B. Shchekin, D. L. Huffaker, and D. G. Deppe, Appl. Phys. Lett. **73,** 3351 (1998).
3. O. B. Shchekin and D. G. Deppe, Appl. Phys. Lett. **80,** 3277 (2002).
4. D. Bimberg, M Grundmann, and N. N. Ledenstov, *Quantum Dot Heterostructures* (Wiley, New York, 1999).
5. F. Klopf, R. Krebs, J. P. Reithmaier, and A. Forchel, IEEE Photonics Technol. Lett. **13,** 764 (2001).
6. A. A. El-Emawy, S. Birudavolu, P. S. Wong, Y. B. Jiang, H. Xu, S. Huang and D. L. Huffaker, J. Appl. Phys. **93,** 3529 (2003).
7. N. N. Ledentsov, M. V. Maximov, D. Bimberg, T. Maka, C. M. Sotomayor Torres, I. V. Kochnev, I. L. Krestnikov, V. M. Lantratov, N. A. Cherkashin and Yu. M. Musikhin, Semicond. Sci. Technol. **15**, 604 (2000).
8. F. Klopf, R. Krebs, J. P. Reithmaier, and A. Forchel, IEEE Photonics Technol. Lett. **13,** 764 (2001)
9. Y. Qiu, P. Gogna, S. Forouhar, A Stintz, and L. F.Lester, Appl. Phys. Lett. **79,** 3570 (2001)
10. H. Chen, Z Zou, OB Shchekin, and D. G. Deppe, Electron. Lett. **36,** 1703 (2000).
11. P. J. A. Thijs, L. F. Tiemeijer, J. J. M. Binsma, and T. van Dongen, IEEE J. Quantum Electron. **30,** 477 (1994).
12. B. I. Miller, U. Koren, M. G. Young, and M. D. Chien, Appl. Phys. Lett. **58,** 1952 (1991)..
13. G. Zhang and A. Ovtchinnikov, Appl. Phys. Lett. **62,** 1644 (1993).
14. A. A. El-Emawy, S. Huang, Y. B. Jiang, C. P. Hains, and D. L. Huffaker, , Appl. Phys. Lett. **87,** 113105 (2005).
15. N. Nuntawong, Y.C. Xin, S. Birudavolu, P.S. Wong, S. Huang, C. P. Hains and D. L. Huffaker, Appl. Phys. Lett. **86,** 193115 (2005).
16. A. L. Gray, Ph.D. dissertation, The American University, 2000.
17. N. Nuntawong, S. Birudavolu, C. P. Hains, S. Huang, H. Xu and D. L. Huffaker, Appl. Phys. Lett. **85,** 3050 (2004).
18. L. Nasi, C. Ferrari, L. Lazzarini and G. Clarke, J. Appl. Phys. **92,** 7678(2002).
19. S. Huang, N. Nuntawong, C. P. Hains and D. L. Huffaker (unpublished)
20. N. Liu, C. K. Shih, J. Geisz, A. Mascarenhas, and J. M. Olson, Appl. Phys. Lett. **73**, 1979 (1998).
21. H. J. Chen, R. M. Feenstra, R. S. Goldman, C. Silfvenius, and G. Landgren, Appl. Phys. Lett. **72,** 1727 (1998).
22. D. L. Huffaker and D. G. Deppe, Appl. Phys. Lett. **73,** 366 (1998).
23. Z.R. Wasilewski, S. Fafard and J. P. McCaffrey, J. Cryst. Growth. **201,** 1131 (1999)
24. S. M. Kim, Y. Wang, M. Keever, and J. S. Harris, IEEE Photonics Technol. Lett. 16, 377(2004)
25. I. N. Kaiander, R. L. Sellin, T. Kettler, N. N. Ledentsov, D. Bimberg, N.D. Zakhorov and P. Werner, Appl. Phys. Lett. **84,** 1024 (2004)
26. G. S. Solomon, M. C. Larson, and J. S. Harris, Appl. Phys. Lett. **69,** 1897 (1996).